Research Paper:

Inocula selection in microbial fuel cells based on anodic biofilm abundance of *Geobacter sulfurreducens*

Guotao Sun (孙国涛)[1], Diogo Rodrigues[1], Anders Thygesen[1#], Geoffrey Daniel[2], Dinesh Fernando[2], Anne S. Meyer[1]

[1] Center for BioProcess Engineering, Department of Chemical and Biochemical Engineering, Technical University of Denmark, Søltofts Plads 229, DK-2800 Kgs. Lyngby, Denmark

[2] Department of Forest Products/Wood Science. Swedish University of Agricultural Science. SE-75007 Uppsala, Sweden.

#Corresponding author: address as above. Telephone no. 0045 21326303, E-mail: athy@kt.dtu.dk

Submission: March 8, 2015, Revision submitted: July 13, 2015.

Abstract

Microbial fuel cells (MFCs) rely on microbial conversion of organic substrates to electricity. The optimal performance depends on the establishment of a microbial community rich in electrogenic bacteria. Usually this microbial community is established from inoculation of the MFC anode chamber with naturally occurring mixed inocula. In this study, the electrochemical performance of MFCs and microbial community evolution were evaluated for three inocula including domestic wastewater (DW), lake sediment (LS) and biogas sludge (BS) with varying substrate loading (L_{sub}) and external resistance (R_{ext}) on the MFC. The electrogenic bacterium *Geobacter sulfurreducens* was identified in all inocula and its abundance during MFC operation was positively linked to the MFC performance. The LS inoculated MFCs showed highest abundance (18 ± 1%) of *G. sulfurreducens*, maximum current density (I_{max}= 690 ± 30 mA·m^{-2}) and coulombic efficiency (CE = 29 ± 1%) with acetate as the substrate. I_{max} and CE increased to 1780 ± 30 mA·m^{-2} and 58 ± 1%, respectively, after decreasing the R_{ext} from 1000 Ω to 200 Ω, which also correlated to a higher abundance of *G. sulfurreducens* (21 ± 0.7%) on the MFC anodic biofilm. The data obtained contribute to understanding the microbial community response to L_{sub} and R_{ext} for optimizing electricity generation in MFCs.

Key words Lake sediment; coulombic efficiency; Denaturing gradient gel electrophoresis; *Geobacter sulfurreducens*; anode polarisation resistance.

1 Introduction

A microbial fuel cell (MFC) encompasses anode and cathode reactions to drive redox processes that result in production of electricity. The core principles of the electricity generation are similar to those in chemical fuel cells, but in MFCs, the reactions rely on bacterial metabolism based on a microbial biofilm on the anode electrode [1]. Fermentative bacteria are needed to convert complex substrates (e.g. glucose) into carboxylic acids including acetate, which can then be digested by electrogenic bacteria [2,3]. *Geobacter sulfurreducens*, is an electrogenic bacterium widely found in nature, which means that it can directly transfer electrons to the electrode [4,5]. The performance of MFCs depends therefore on the type and abundance of the microbial consortium in the anode chamber and notably in the anode biofilm. *The inoculum source of electrogenic and fermentative bacteria is therefore important in the establishment of the anodic biofilm.*

Inocula sources that have been studied in MFCs include pure bacteria [5], domestic wastewater (DW) [6–8] and biogas sludge (BS) [9]. Nevin et al. reported that pure cultures of electrogenic bacteria can produce higher maximum power density (MPD = 1900 $mW \cdot m^{-2}$) than mixed communities (1600 $mW \cdot m^{-2}$) with acetate as feed [5]. Holmes et al. [10] operated MFCs inoculated with marine sediment, salt-marsh sediment and freshwater sediment and showed that the power output was linked to electrogenic bacteria regardless of the salinity. Yates et al. [7] examined the microbial community in two-chamber H-shape MFCs inoculated with DW (two sources tested) and lake sediment (LS). They found that the cell voltage reached similar values (470 ±

20 mV) after 20 operational cycles and that the anodic biofilm community were dominated by *Geobacter* sp.

Previous studies have shown that external resistance (R_{ext}) and substrate concentration affect the power generation and microbial community composition [11–13]. It is known that in a mixed culture, the electrogenic bacteria compete for substrate with the fermentative non-electrogenic bacteria [13]. From the available literature, it is clear that a decaying microbiota is required for the MFC to convert organic substrates to electric current via electrogenic bacteria, but it is unclear whether the frequently tested DW may be surpassed by denser inocula such as BS and LS. A better understanding of the evolution of the electrogenic versus the fermentative non-electrogenic bacteria will aid in improving MFC performance.

The objective of this work is to assess the electrochemical performance, stability and microbial consortium development using three inocula including DW, BS and LS, respectively. It was expected that a denser inoculum would allow an increase in power generation and make the process more robust to substrate changes. Based on the optimal inocula, the effect on the microbial evolution of a variation of R_{ext} and substrate loading (L_{sub}) was examined to improve MFCs performance. The process analysis was performed with thorough microbial analysis, and chemical analysis and electrochemical impedance spectroscopy (EIS).

2 Materials and methods

2.1 MFCs configuration

The H-shaped reactors used in this study were constructed by two cylindrical acrylic glass bottles with a volume of 300 cm^3 for each of the compartments (220 cm^3 liquid), which were connected with a tube with an inner diameter of 30 mm [6]. A proton exchange membrane (Nafion™ N117, Dupont Co., USA) with an area of 7.1 cm^2 was placed between the chambers. The two chambers were tightened with rubber rings. Both anode and cathode electrode were made of two paralleled carbon paper sheets (TGPH-020, Fuel Cells Etc, USA) of 3 cm × 8 cm (A = 24 cm^2) and a thickness of 0.35 mm.

2.2 Inoculation and operational conditions

The basic anolyte consisted of M9 medium containing per liter: 6 g Na_2HPO_4, 3 g KH_2PO_4, 1 g $NaHCO_3$, 1 g NH_4Cl, 0.5 g NaCl, 0.247 g $MgSO_4 \cdot 7H_2O$, 0.0147 g $CaCl_2$ and 1 cm^3 trace element solution [6]. pH could be maintained at 7.0 due to the high buffer capacity of the M9 medium (64 $mmol \cdot dm^{-3}$ of phosphate buffer + 12 $mmol \cdot dm^{-3}$ of carbonate buffer). The carbon source (sodium acetate or xylose) was added to the medium. The cathode solution was 100 $mmol \cdot dm^{-3}$ of $K_3Fe(CN)_6$ and 100 $mmol \cdot dm^{-3}$ of phosphate buffer (pH 6.7) and was replaced at the beginning of each cycle. All MFCs were operated at 30 ℃ in an incubator with magnetic stirring [6].

Reactors (triplicates) were inoculated with three types of inocula: DW obtained after the fine separation process (Lyngby Taarbæk Community, Denmark); LS collected from Sorø lake (55º25´21"N, 11º32´23"E); and BS from Hashøj Biogas (Dalmose,

Denmark). pH, electric conductivity (EC), dry matter (DM) and chemical oxygen demand (COD) of these inocula are shown in Table 1. The reactors were inoculated in a 1:1 ratio of medium to inocula and fed with sodium acetate (1 $g \cdot dm^{-3}$ of COD) using R_{ext} of 1000 Ω. Feeding was done every 5 days (equal to one cycle) with fresh medium and corresponding substrates. Due to start up time, the first cycle lasted for 7 days. After 2 to 3 batch cycles, stable power generation was obtained in all the reactors. The acetate substrate was changed to xylose to study the adaptability of the microbial community to a fermentative substrate still using 1 $g \cdot dm^{-3}$ of COD content.

Based on the inocula test, four reactors (duplicate) inoculated with an optimal inoculum (LS) were operated in batch mode testing R_{ext} of 200, 500, 800 and 1000 Ω. Anode solution was replaced every 5 days, which equals to one cycle. From second cycle, all the reactors were fed with fresh medium and sodium acetate. After 3 batch cycles, stable power generation was obtained and different L_{sub} (0.5, 1, 1.5 and 2 $g \cdot dm^{-3}$ of COD) were tested in the MFCs. Operational cycles and corresponding R_{ext} and L_{sub} are outlined in Table 2.

2.3 Microbial community analysis

Biofilm samples from the anode chamber were obtained by cutting 0.5 cm^2 of the anode electrode surface at the end of each cycle [6]. Genomic DNA extraction followed by polymerase chain reaction (PCR) and denaturing gradient gel electrophoresis (DGGE) were conducted as previously described [6,14]. Similarity between the samples was analyzed by using BioNumerics software v.7.1 (Applied Maths, Sint-Martens Latem, Belgium) [6].

A clone library for providing a phylogenetic affiliation of the DGGE bands was constructed and resulting sequences were submitted to EMBL Nucleotide Sequence

Database (Accession No. LN650984 – LN651064). Subsequently the unique clones were amplified by PCR as described above. The PCR products were then run in a DGGE gel to identify the bands formed by biofilm samples [6].

2.4 Scanning electron microscopy

In order to examine biofilms on the anode surfaces, the anodic electrode (~ 1 cm^2) was removed without touching its surface. Small samples (1 × 1 cm) were fixed in 50 $dm^3 \cdot m^{-3}$ glutaraldehyde + 20 $dm^3 \cdot m^{-3}$ paraformaldehyde in 0.1 $mol \cdot dm^{-3}$ Na-acetate in deionized water (pH 7.2). After fixation, the samples were dehydrated in aqueous ethanol using: 20%, 40%, 60%, 80%, 90% and 100% for 20 min in each solution. Subsequent dehydration was performed in 33%, 66% and 100% acetone in ethanol before samples were critical point dried using Agar E3000 critical point dryer (Agar Scientific, Stansted, UK) with liquid CO_2 as drying agent. Following coating with gold using an Emitech E5000 sputter coater, samples were observed using a Philips XL30 ESEM scanning electron microscope at 50 to 10000 times of magnification [15].

2.5 Chemical, electrochemical and statistical analysis

The COD concentration and dry matter content were measured similar to Sun et al. [6]. Concentrations of monomeric sugars and volatile fatty acids (VFA) were measured by HPLC (High-performance liquid chromatography) [6]. pH and electrical conductivity were tested by multimeter (Multi 3430, WTW, Germany).

Electric current was recorded every 15 minutes by a data logger (Model 2700, Keithley Inc.). In polarization tests, R_{ext} was varied between 30 Ω and 50 kΩ. The current density (I) and maximum current density (I_{max}) were calculated by dividing the current with the electrode surface area (A = 48 cm^2) including both sides. EIS was

carried out with a potentiostat (SP-150, BioLogic, France). The anode polarization resistance was measured by connecting the MFCs to the potentiostat in the three-electrode mode within the range from 10 kHz to 0.1 Hz with amplitude of 10 μA. Lower frequencies were not tested since it can disturb the microbial process due to a long test period (> 1 h). The anode and cathode were used as working electrode and counter electrode, respectively. The third lead was attached to a reference electrode (Ag/AgCl; #MF2079; Bioanalytical Systems Inc.) inserted in the anode chamber. Zview (Scribmer Associates Inc.) was used for EIS data fitting. Coulombic efficiency (CE) was calculated as the ratio of accumulative charges produced from the MFCs to the charges released from substrate degradation. Statistics analysis by ANOVA (one-way; $p<0.05$) was done by using Minitab 16 and means were compared using Turkey's multiple range procedure. The significant difference between the values was indicated by letters A–D.

3 Results and discussion

3.1 Electricity generation in MFCs using the three inocula

The current density outputs of the DW-, LS- and BS- inoculated MFCs are shown in Fig. 1. During cycle 1, DW-inoculated MFCs needed shorter lag time (2 days) to achieve stable current than LS-inoculated MFCs (4 days) and BS-inoculated MFCs (5 days). The short lag time of DW-inoculated MFCs indicated rapid start-up compared with previous studies of 7 days by Li et al. [16] and 9.5 days by Zhang et al. [8]. After 2 cycles of MFC operation, the average current density (I_{ave}=138 ± 2 mA·m^{-2}) in LS-inoculated MFCs was slightly higher (2 – 5 %) than in DW- and BS-inoculated MFCs. When xylose was added to all the MFCs (cycle 3), they took one day to recover to stable current generation. Adaptation of the MFCs to xylose also resulted in a 20% drop

in I_{ave}. In particular for DW-inoculated MFCs (Fig. 1A), I_{ave} showed earlier drop at the end of cycles 4 and 5, but after 3 cycles, all MFCs converged to a similar I_{ave} (140 ± 2 mA·m^{-2}). *Thereby DW showed the shortest lag time while LS gave the highest I_{ave}. However, I_{ave} was similar with the three inocula after shifting to xylose (cycle 5).*

I_{max} is a key factor demonstrating the capability of power generation that MFCs can produce (Table 3). I_{max} in all the MFCs increased from cycles 2 to 6, which can be explained by the study of Read et al. [3] showing that a stronger biofilm can be formed when the MFCs run for longer time. With acetate, LS-inoculated MFCs showed the highest I_{max} (cycle 3; 690 ± 30 mA·m^{-2}) compared with DW (440 ± 50 mA·m^{-2}) and BS (370 ± 30 mA·m^{-2}). After addition of xylose (cycle 6), LS-inoculated MFCs still generated higher I_{max} (1690 ± 40 mA·m^{-2}), than DW and BS with 1330 ± 10 and 930 ± 50 mA·m^{-2}, respectively. *The differentiation in I_{max} proved that the inocula had a significant effect on electricity generation and that LS-inoculated MFCs performed best.*

3.2 Substrate conversion and efficiency using the three inocula

For the acetate fed MFCs, the utilisation of acetate and current generation are shown in Fig 2A,B,C (cycle 3). Acetate removal rates in the range of 58 – 61% were achieved after 5 days of current generation (I_{ave} = 131 – 138 mA·m^{-2}) with the three inocula. For the xylose fed MFCs, the utilisation of xylose and formation of acetate and propionate are shown in Fig 2D,E,F (cycle 5). Xylose was completely degraded with all the inocula after the first day with accumulation of acetate and propionate as by-products. The accumulation of acetate (5.2 ± 0.2 mmol·dm^{-3}) in DW-inoculated MFCs was higher than with LS (4.7 ± 0.4 mmol·dm^{-3}) and with BS (3.7 ± 0.2 mmol·dm^{-3}). *The high formation of acetate with DW indicates a large abundance of xylose-fermenting*

bacteria since acetate is produced faster than it is utilized in the electrogenic bacteria [2].

CE was calculated based on the accumulated charge produced from the MFCs divided by the charge released from substrate degradation as shown in Table 3. LS showed the highest CE of 29 ± 1% when acetate was used (cycle 3). The higher CE is due to the high current density and low COD removal. After xylose was added to the MFCs (cycle 4), CE dropped dramatically to 14 ± 2%, 18 ± 1% and 17 ± 0.1% for DW, LS and BS, respectively. However, the CE increased to 17 ± 3%, 23 ± 1% and 21 ± 1% respectively after 3 cycle of operation (cycle 6). *The highest CE (23%) and I_{max} (1690 $mA \cdot m^{-2}$) were thereby obtained in the LS-inoculated MFCs.*

3.3 Anode polarization resistance using the three inocula

In an MFC, the biofilm, which is attached to the anode, serves as biocatalyst for electricity generation. The metabolism of bacteria in MFCs is one of the limiting factors for power generation which can be represented by the polarisation resistance of the anode. EIS is an efficient non-destructive technique to determine the anode polarisation resistance [17]. Measurements were conducted by connecting the MFC to a potentiostat in three-electrode mode. The impedance of the anode is presented in Fig. 3 and was used to calculate anode polarisation resistance (R_p) by fitting the impedance data to Randles circuit (Fig. 3D). The anode polarisation resistance for DW-, LS- and BS-inoculated MFCs were 94 Ω, 119 Ω and 87 Ω, respectively, before MFCs started work. The differentiation of the resistance at this time is due to the different EC in the inocula (Table 1). Resistance decreased after the MFCs achieved stable current generation to 51

Ω (DW), 30 Ω (LS) and 40 Ω (BS), respectively. The decrease in resistance indicated that the biofilm formed on the anode surface activated the electrochemical reaction and that LS-inoculated MFCs can generate higher I_{max} than DW and BS. Furthermore, when the more complicated substrate (xylose) was added to all the MFCs, LS-inoculated MFCs performed with lower anode resistance (24 Ω) than DW (41 Ω) and BS (35 Ω). *These results are corroborated by Fan et al. [18] that the lower anode resistance with LS contribute to higher power generation (Table 3).*

3.4 Effects of R_{ext} and L_{sub} on electricity generation

Four MFCs (duplicate), with a different R_{ext} (200, 500, 800 and 1000 Ω), were evaluated from cycle 1 to 3 for I_{ave} and I_{max} (Table 4). The reactors with 200 Ω needed 1.5 days before notable current generation was obtained, while the reactors at 500 – 1000 Ω needed 2.5 days. The MFCs with lower R_{ext} performed thereby a better start-up in agreement with a previous study [10]. After stable current was observed, I_{ave} ranged from 145 ± 10 mA·m^{-2} (1000 Ω) to 555 ± 8 mA·m^{-2} (200 Ω). Differences of I_{max} among these reactors with different R_{ext} were also noted. The MFCs with 200 Ω produced highest I_{max} of 1780 ± 30 mA·m^{-2}, while 1000 Ω only generated 570 ± 0.01 mA·m^{-2}. After all MFCs changed to use 200 Ω (cycle 4), similar I_{ave} (557 ± 13 mA·m^{-2}) and I_{max} (1800 ± 20 mA·m^{-2}) were generated. At R_{ext} of 200 Ω (cycle 5), the L_{sub} showed no significant effect on I_{ave} and I_{max} excepting the L_{sub} of 0.5 g COD·dm^{-3}, which generated lower I_{ave} (419 ± 28 mA·m^{-2}) than the higher L_{sub} (555 mA·m^{-2}). This can be explained by previous research, which reported that only at low resistances or at near maximum current the increased L_{sub} can result in increased electricity generation [10].

Table 4 also reported COD removal rate (COD_{rr}) and CE in the MFCs with different R_{ext} and L_{sub}. The MFCs with lower R_{ext} showed both higher COD_{rr} (152 ± 1 $g \cdot m^{-3} \cdot day^{-1}$) and higher CE (58 ± 1%), which can be attributed to the higher rate of elecrogenesis resulting in higher current generation. Comparatively, the decreasing L_{sub} resulted in lower COD_{rr} (92 ± 6 $g \cdot m^{-3} \cdot day^{-1}$) and higher CE (61 ± 2%). A previous study, using the same MFC design, also reported that the increasing L_{sub} from 0.25 to 2 $g \cdot dm^{-3}$ of COD resulted in a decrease of CE from 37% to 16% [19]. *High I_{ave} and high CE were thereby obtained at low* R_{ext} *(200 Ω) and a relatively low L_{sub} of 1 $g \cdot dm^{-3}$ of COD.*

3.5 Microbial community: effect of inocula

3.5.1 Biofilm microstructure

SEM analysis of the micro- and ultrastructure of anode electrode biofilms after the 6 cycles of MFC operation showed considerable differences as shown in Fig 4. The control showed no bacterial colonisation over the surface of the electrodes (Fig. 4a). The electrode rods had clean, smooth and homogeneous surfaces (Fig. 4a, inset top right) with even diameter of ca 8 μm. BS: Not dense unevenly distributed bacteria and only low biofilm slime formation was observed (Fig. 4b). Sometimes, rods were observed with areas of non-colonized clear surfaces (Fig. 4b, inset top right). In addition, a diverse bacterial community (e.g. long rod types (arrowhead, Fig. 4c) and oval shaped ones (arrows, Fig. 4c)) was apparent (Fig. 4c).These characteristics agree the low I_{max} of 930 $mA \cdot m^2$ (Table 3). DW: Electrode rods had unclean surfaces with often observed inhomogeneous particles (arrows, Fig. 4d). A close-up view showed condensed colonies of mostly rod shaped bacteria with infrequent presence of slimy

material (inset top right, Fig. 4d and Fig. 4e). Different bacterial morphology was found (Fig. 4f) and the bacteria were attached to each other (Fig. 4e and 4f). In addition, it was also infrequently observed nano-threads like structures from bacteria (arrows, Fig. 4g) and all these characteristics of the biofilm should collectively contribute to the 43% higher I_{max} (Table 3).

LS: An even higher and thick colonisation of the electrode surfaces were seen (Fig. h) with more frequent particles of varying sizes densely distributed over electrodes (arrows, Fig. 4h). The large particles were thick highly concentrated bacterial colonies (inset top right, Fig. 4h) that are thought to contribute for higher electricity production. In addition, morphology of the biofilm indicated comparatively less diverse bacterial communities where long rod-shaped bacteria were more commonly observed (Fig, 4i). Interestingly, nano threads-like appendages ranging from 70-120 nm in width and extending tens of micron long were often seen associated with rod-shaped bacteria (arrowheads, Fig. 4j) presumably representing bacterial nanowires. *G. sulfurreducens* are known to produce nanowires that are highly conductive and have potential for long-range exocellular electron transfer across biofilm via intertwined nanowires [20,21]. These characteristics lead to 82% higher I_{max} than with BS (Table 3) and presumably also suggest high abundance and activity of electrogenic *Geobacter* sp. as evidence from DGGE analysis (Fig. 5).

3.5.2 Molecular determination of microbial community

In order to provide greater insight into microbial diversity of the biofilm samples, bacterial gene libraries were examined using full length 16S rRNA (Table 5). The bacterial species identified included the electrogenic species *G. sulfurreducens* [5] and

the fermenting species *Bacteroides graminisolvens* [22], *Arcobacter butzleri* [23], *Paludibacter propionicigenes* [24], *Thermanaerovibrio acidaminovorans* [25], *Enterobacter cancerogenus* [26], *Citrobacter braakii* [27] and *Propionispora hippie* [28].

The anodic biofilms in the three types of inoculated MFCs were sampled at the end of each batch test (from cycle 2 to 5) as shown in Fig. 1. The microbial community of the biofilm samples were analysed with 16S rRNA-based DGGE in combination with a clone library as summarized in Fig. 5A. The band patterns of the biofilm in all the MFCs became stable after 7 days of enrichment with inocula and acetate (cycle 1 in Fig. 1). The similarities between the lanes comparing cycle 2 and 3 were higher than 88% for the 3 inocula. However, the band patterns in cycle 2 varied significantly between the three types of inoculated MFCs with 59% for LS compared to DW (LS_2:DW_2) and with 33% for LS compared to BS (LS_2:BS_2). The patterns of the bands also changed after switching substrate from acetate to xylose in all the MFCs, with similarities from cycle 3 to 4 of 46%, 40% and 4% for LS, DW and BS, respectively. After short acclimation of the MFCs to xylose, stable band patterns were observed in all the biofilm samples with similarities above 80% (LS_4, LS_5; DW_4, DW_5; and BS_4, BS_5). *The distinct similarities among the different inocula and substrates demonstrated that they are key factors affecting anodic microbial community in MFCs.*

When acetate was used in MFCs, *G. sulfurreducens* was predominant with all the inocula. In addition, *T. acidaminovorans* was dominant with DW, *Shigella flexneri* and *Azonexus caeni* were dominant with LS and *S. flexneri* was dominant with BS (comparing cycle 2 and 3). Among these species, only *G. sulfurreducens* has the potential to electricity generation as a metal-reducing bacterium [4,5,29]. The change to

use xylose resulted also in a more diverse microbial community. LS-inoculated MFCs became dominated by *E. cancerogenus*, *G. sulfurreducens*, *C. braakii* and *P. hippie*. *The presence of a more diverse microbial community after addition of xylose further illustrated why it took a short adaptation time for the MFCs to enrich fermentative bacteria to convert complex substrates (xylose) to non-fermentable substrates (e.g. acetate and propionate) [8]*.

3.5.3 Quantification of G. sulfurreducens

Composite analysis of the DGGE bands showed the different proportions of *G. sulfurreducens* in the biofilm community (Fig. 5B). When acetate was added to MFCs (cycle 2), LS-inoculated MFCs had the highest percentage of *G. sulfurreducens* (18 ± 1%) compared to DW and BS with 12 ± 0.4% and 11 ± 3%, respectively. The high proportion of *G. sulfurreducens* in LS-inoculated MFCs may further explain the higher I_{max} generation (Table 3). These results are also corroborated by Li et al. showing that DW-inoculated MFCs produced much higher MPD (33 $mW \cdot m^{-2}$) than activated sludge inoculated MFCs (23 $mW \cdot m^{-2}$) with the predominance of *Geobacter pickeringii* and *Magnetospirillum* sp. in the wastewater inoculated MFCs [16]. However, the abundance of these species was not quantified.

After xylose was added to the MFCs (cycle 4), the proportion of *G. sulfurreducens* decreased to 6 – 11%. This may be due to that xylose boosts the growth of fermentative bacteria, which also resulted in a significant drop in CE (Table 3). However, the concentration of *G. sulfurreducens* increased after two cycles of MFC operation to 13 ± 0.3% in LS-inoculated MFCs, which was higher than DW (11 ±0.2%) and BS (10 ± 0.3%). *These results show that I_{max} increased versus the abundance of electrogenic bacteria (most G. sulfurreducens* with the LS inoculum).

3.6 Effects of R_{ext} and L_{sub} on microbial community and current generation

Based on DGGE band intensities in Fig 6A, the abundance of *G. sulfurreducens* in the biofilm communities was estimated (Fig. 6B). After 3 batches, the MFCs with R_{ext} of 200-Ω showed highest proportion of *G. sulfurreducens* (21 ± 0.7%), followed by 18 ± 0.4%, 16 ± 0.4% and 16 ± 0.4% for 500-, 800- and 1000 Ω, respectively. The higher abundance of *G. sulfurreducens* in 200-Ω MFCs explains why they generated higher I_{max} and CE (Table 4). The results also indicated that the lower R_{ext} assist the enrichment of *G. sulfurreducens*, as explained as that lower R_{ext} results in higher electrode potential [11], which is favoured by *G. sulfurreducens* growth. When all MFCs changed to use R_{ext} of 200 Ω, no significant difference in the proportion of *G. sulfurreducens* (22 – 23 %) was observed.

The increase in MFC performance versus the abundance of the *G. sulfurreducens* is also reflected by I_{ave} in the MFCs with different L_{sub} (Table 4). The maximum I_{ave} was 557 ± 13 mA·m^{-2} at 200 Ω, which is almost two times higher than I_{ave} (285 ± 6 mA·m^{-2}) at 150 Ω reported by Jung and Regan [13]. Whereas an increase in the L_{sub} from 0.5 to 1.0 g·dm^{-3} of COD had no measureable effect on the abundance of the *G. sulfurreducens*. In general, increased L_{sub} significantly decreased the abundance of *G. sulfurreducens* (20% →12%) (Fig. 6B). The increased L_{sub} boosted thereby enrichment of fermenting bacteria, which in turn significantly decreased CE. The increased abundance of *G. sulfurreducens* resulted in an increase of CE regardless of the level of R_{ext} and L_{sub}, which demonstrated that CE increased versus the abundance of electrogenic bacteria. *The results show that low R_{ext} and low L_{sub} increased the abundance of G. sulfurreducens, which in turn gave higher I_{ave}.*

Overall SEM microscopy (Fig. 4) showed dense, less diverse and highly active bacterial community and DGGE showed high dominance of *G. sulfureducens* for the LS inoculum (Fig. 5). Both of these results confirm the hypothesis that high current generation is linked to high dominance of *G. sulfureducens* (Table 3).

4 Conclusion

This study showed that the lake sediment inoculated MFCs yielded higher I_{max} up to 1690 mA·m^{-2} and CE up to 23 ± 1% at R_{ext} of 1000 Ω. A decrease of R_{ext} significantly increased I_{max} and CE to 1800 mA·m^{-2} and 59 ± 1%, respectively, while an increase of L_{sub} only showed effect on CE with a decrease. On the basis of electrochemical performance and microbial community analysis, the higher abundance of *G. sulfurreducens* resulted in higher MFCs performance with emphasis on current generation and coulombic efficiency. Elucidating the positive correlation between microbial community and electrochemical performance will assist in optimization of MFCs technology for practical application.

Acknowledgement

The authors are grateful to Danida Fellowship Centre for supporting the research project (Biobased electricity in developing countries, DFC No. 11–091 Risø). The financial support from China Scholarship Council (CSC No. 2011635051) for Guotao Sun is gratefully acknowledged.

Reference

[1] Sun, G., Thygesen, A., Ale, M.T., Mensah, M., Poulsen, F.W., Meyer, A.S., "The significance of the initiation process parameters and reactor design for maximizing the efficiency of microbial fuel cells", *Appl. Microbiol. Biotechnol.*, **98**, 2415–2427 (2014).

[2] Lovley, D.R., "Microbial fuel cells: novel microbial physiologies and engineering approaches", *Curr. Opin. Biotechnol.*, **17**, 327–332 (2006).

[3] Read, S.T., Dutta, P., Bond, P.L., Keller, J., Rabaey, K., "Initial development and structure of biofilms on microbial fuel cell anodes", *B.M.C. Microbiol.*, **10**, 98 (2010).

[4] Lovley, D.R., Phillips, E.J.P., "Novel mode of microbial energy metabolism : organic Carbon oxidation coupled to dissimilatory reduction of iron or manganese", *Appl. Environ. Microbiol.*, **54**, 1472–1480 (1988).

[5] Nevin, K.P., Richter, H., Covalla, S.F., Johnson, J.P., Woodard, T.L., Orloff, A.L., Jia, H., Zhang, M., Lovley, D.R., "Power output and columbic efficiencies from biofilms of *Geobacter sulfurreducens* comparable to mixed community microbial fuel cells", *Environ. Microbiol.*, **10**, 2505–2514 (2008).

[6] Sun, G., Thygesen, A., Meyer, A.S., "Acetate is a superior substrate for microbial fuel cells initiation utilizing bioethanol effluent", *Appl. Microbiol. Biotechnol.*, **99**, 4905-4915 (2015).

[7] Yates, M.D., Kiely, P.D., Call, D.F., Rismani-Yazdi, H., Bibby, K., Peccia, J., Regan, J.M., Logan, E.B., "Convergent development of anodic bacterial communities in microbial fuel cells", *I.S.M.E. J.*, **6**, 2002–2013 (2012).

[8] Zhang, Y., Min, B., Huang, L., Angelidaki, I., "Electricity generation and microbial community response to substrate changes in microbial fuel cell", *Bioresour. Technol.*, **102**, 1166–1173 (2011).

[9] Chae, K.J., Choi, M.J., Lee, J.W., Kim, K.Y., Kim, I.S., "Effect of different substrates on the performance, bacterial diversity, and bacterial viability in microbial fuel cells", *Bioresour. Technol.*, **100**, 3518–3525 (2009).

[10] Holmes, D.E., Bond, D.R., O'Neil, R.A., Reimers, C.E., Tender, L.R., Lovley, D.R., "Microbial communities associated with electrodes harvesting electricity from a variety of aquatic sediments", *Microb. Ecol.*, **48**, 178–190 (2004).

[11] Aelterman, P., Versichele, M., Marzorati, M., Boon, N., Verstraete, W., "Loading rate and external resistance control the electricity generation of microbial fuel cells with different three-dimensional anodes" *Bioresour. Technol.*, **99**, 8895–8902 (2008).

[12] Jadhav, G.S., Ghangrekar, M.M., "Performance of microbial fuel cell subjected to variation in pH, temperature, external load and substrate concentration", *Bioresour. Technol.*, **100**, 717–723 (2009).

[13] Jung, S., Regan, J.M., “Influence of external resistance on electrogenesis, methanogenesis, and anode prokaryotic communities in microbial fuel cells”, *Appl. Environ. Microbiol.*, **77**, 564–571 (2011).

[14] Muyzer, G., de Waal, E.C., Uitterlinden, A.G., “Profiling of complex microbial populations by denaturing gradient gel electrophoresis analysis of polymerase chain reaction-amplified genes coding for 16S rRNA”, *Appl. Environ. Microbiol.*, **59**, 695–700 (1993).

[15] Thygesen, A., Daniel, G., Lilholt, H., Thomsen, A.B., “Hemp fiber microstructure and use of fungal defibration to obtain fibers for composite materials”, *J. Nat. Fibers*, **2**, 19–37 (2005).

[16] Li, X.M., Cheng, K.Y., Selvam, A., Wong, J.W.C., “Bioelectricity production from acidic food waste leachate using microbial fuel cells: effect of microbial inocula”, *Process. Biochem.*, **48**, 283–288 (2013).

[17] Ter Heijne, A., Schaetzle, O., Gimenez, S., Fabregat-Santiago, F., Bisquert, J., “Strik DPBTB, Barriere F, Buisman CJN, Hamelers HVM. Identifying charge and mass transfer resistances of an oxygen reducing biocathode”, *Energy Environ. Sci.*, **4**, 5035-5043 (2011).

[18] Fan, Y., Sharbrough, E., Liu, H., “Quantification of the internal resistance distribution of microbial fuel Cells”, *Environ. Sci. Technol.*, **42**, 8101–8107 (2008).

[19] Zhang, Y., Min, B., Huang, L., Angelidaki, I., “Generation of electricity and analysis of microbial communities in wheat straw biomass-powered microbial fuel cells”, *Appl. Environ. Microbiol.*, **75**, 3389–3395 (2009).

[20] Logan, B.E., Regan, J.M., “Electricity-producing bacterial communities in microbial fuel cells”, TRENDS in Microbiol., 14, 512-518 (2006).

[21] Reguera, G., Nevin, K.P., Nicoll, J.S., Covalla, S.F., Woodard, T.L., Lovley, D.R., “Biofilm and Nanowire Production Leads to Increased Current in *Geobacter sulfurreducens* Fuel Cells”, Appl. Environ. Microbiol., 72, 7345–7348 (2006).

[22] Nishiyama, T., Ueki, A., Kaku, N., Watanabe, K., Ueki, K., “*Bacteroides graminisolvens* sp. nov., a xylanolytic anaerobe isolated from a methanogenic reactor treating cattle waste”, *Int. J. Syst. Evol. Microbiol.*, **59**, 1901-1907 (2009).

[23] Rice, E.W., Rodgers, M.R., Wesley, I.V., Johnson, C.H., Tanner, S., “Isolation of *Arcobacter butzleri* from ground water”, *Lett. Appl. Microbiol.*, **28**, 31–35 (1999).

[24] Ueki, A., Akasaka, H., Suzuki, D., Ueki, K., “*Paludibacter propionicigenes* gen. nov., sp. nov., a novel strictly anaerobic, Gram-negative, propionate-producing bacterium isolated from plant residue in irrigated rice-field soil in Japan”, *Int. J. Syst. Evol. Microbiol.*, **56**, 39-44 (2006).

[25] Chovatia, M., Sikorski, J., Schröder, M., Lapidus, A., Nolan, M., Tice, H., Glavina, Del Rio, T., Copeland, A., Cheng, J.F., Lucas, S., Chen, F., Bruce, D.,

Goodwin, L, Pitluck, S., Ivanova, N., Mavromatis, K., Ovchinnikova, G., Pati, A., Chen, A., Palaniappan, K., Land, M., Hauser, L., Chang, Y.J., Jeffries, C.D., Chain, P., Saunders, E., Detter, J.C., Brettin, T., Rohde, M., Göker, M., Spring, S., Bristow, J., Markowitz, V., Hugenholtz, P., Kyrpides, N.C., Klenk, H.P., Eisen, J.A., "Complete genome sequence of *Thermanaerovibrio acidaminovorans* type strain (Su883)", *Stand. Genomic. Sci.*, **1**, 254-261 (2009).

[26] Kazaks, A., Dislers, A., Lipowsky, G., Nikolajeva, V., Tars, K., "Complete Genome Sequence of the *Enterobacter cancerogenus* Bacteriophage Enc34", *J. Virol.*, **86**, 11403-11404 (2012).

[27] Brenner, D.J., O'Hara, C.M., Grimont, P.A.D., Janda, J.M., Falsen, E., Aldova, E., Ageron, E., Schindler, J., Abbott, S.L., Steigerwalt, A.G., "Biochemical identification of *Citrobacter* species defined by DNA hybridization and description of *Citrobacter gillenii* sp. nov. (formerly *Citrobacter* genomospecies 10) and *Citrobacter murliniae* sp. nov. (formerly *Citrobacter* genomospecies 11)", *J. Clin. Microbiol.*, **37**, 2619-2624 (1999).

[28] Abou-Zeid, D.M., Biebl, H., Sproer, C., Muller, R.J., "*Propionispora hippei* sp nov., a novel Gram-negative, spore-forming anaerobe that produces propionic acid", *Int. J. Syst. Evol.*, **54**, 951-954 (2004).

[29] Liu, Y., Harnisch, F., Fricke, K., Sietmann, R., Schröder, U., "Improvement of the anodic bioelectrocatalytic activity of mixed culture biofilms by a simple consecutive electrochemical selection procedure", *Biosens. Bioelectron.*, **24**, 1012–1017 (2008).

Captions of the Figures

Fig. 1. Current density in MFCs inoculated with DW (A), LS (B) and BS (C) respectively. ace: acetate; xyl: xylose. The arrows indicate the substrate replacement. pH was found constant on approx. 7 during the experimental cycles.

Fig. 2. I_{ave} and substrate degradation as function of time in MFCs enriched with DW (A, D), LS (B, E) and BS (C, F) respectively. The substrate used in (A, B, C) and (D, E, F) are acetate and xylose, respectively. The initial concentration for each substrate was 1 $g \cdot dm^{-3}$ of COD.

Fig. 3. The impedance of the anode in MFCs inoculated with DW, LS and BS respectively. (A) Beginning MFC operation; (B) MFCs using acetate as substrate; (C) MFCs using xylose as substrate. (D) Schematic of Randles equivalent circuit to model charge transfer: ohmic resistance (R_s), polarisation reisitance (R_p) and constant phase element (CPE).

Fig. 4. Scanning electron micrographs of the electrode without biofilm (a) and electrodes in MFCs showing their micro- and ultrastructure of biofilms formed after inoculated with BS (b, c), DW (d-g) and LS (h-j), respectively. Bars: a,b,d,h, 100 µm; c, 3 µm; e, 10 µm; f,g,i,j, 2 µm.

Fig. 5. Bacterial 16S rRNA gene-derived DGGE profiles (A) and relative abundance of *G. sulfurreducens* in MFCs inoculated with DW, LS and BS respectively (B). The numbers (2, 3, 4 and 5) in lanes name (DW_2, DW_3, ……, BS_4, BS_5) means the samples were taken at the end of 2nd, 3rd, 4th and 5th cycle, respectively. The identified bands (1-11) are presented in table 4. UB indicates bands not identified by cloning. Letters A–C indicates significant difference at 95% confidence limit.

Fig. 6. Bacterial 16S rRNA gene-derived DGGE profiles (A) and relative abundance of *G. sulfurreducens* with different R_{ext} and L_{sub} (B). The letter a – d indicating the

MFCs started with 200, 500, 800 and 1000 Ω respectively. The numbers (3, 4 and 5) in lanes name (a_3, a_4, ……, c_5, d_5) means the sample were taken at end of the batch cycle 3, 4 and 5 respectively. The identified bands (1-11) are presented in Table 4. UB indicates bands not identified by cloning. Letters A–C indicates significant difference.

Table 1 Chemical parameters of the inocula including pH, electric conductivity (EC), dry matter (DM) and chemical oxygen demand (COD).

Inocula	pH	EC [$mS \cdot cm^{-1}$]	DM [$mg \cdot g^{-1}$]	COD [$g \cdot dm^{-3}$]
DW	7.2	2.1	1.2	0.4
LS	7.4	0.9	3.8	2.1
BS	8.2	37.0	20.5	16.5

Table 2 Overview of the operational parameters in 4 MFCs (duplicates) testing R_{ext} and L_{sub}.

Batch No.	R_{ext} [Ω]	COD conc (L_{sub}) [g·dm^{-3}]
Cycle 1	200, 500, 800 and 1000	1
Cycle 2	200, 500, 800 and 1000	1
Cycle 3	200, 500, 800 and 1000	1
Cycle 4	200	1
Cycle 5	200	0.5, 1, 1.5 and 2
Cycle 6	200	0.5, 1, 1.5 and 2

Table 3 I_{max} and CE generated in MFCs inoculated with DW, LS and BS respectively. Batch No. is corresponding to the batch test in Fig. 1. Letters A–D indicates column wise significant difference.

Batch No.	I_{max} [mA·m^{-2}]			CE [%]		
	DW	LS	BS	DW	LS	BS
Cycle 2	390 ± 10 ^{A}	410 ± 30 ^{A}	390 ± 10 ^{A}	28 ± 2^{A}	31 ± 4 ^{A}	23 ± 2 ^{AB}
Cycle 3	440 ± 50 ^{AB}	690 ± 30 ^{A}	370 ± 30 ^{A}	27 ± 1^{A}	29 ± 1^{AB}	24 ± 1^{B}
Cycle 4	580 ± 90 ^{BC}	680 ± 20 ^{BC}	590 ± 70 ^{A}	14 ± 2^{B}	18 ± 1^{C}	17 ± 0.1^{B}
Cycle 5	840 ± 20 ^{C}	1000 ± 60 ^{C}	870 ± 50 ^{A}	19 ± 3^{B}	22 ± 0.5^{BC}	21 ± 1^{AB}
Cycle 6	1330 ± 10 ^{D}	1690 ± 40 ^{C}	930 ± 50 ^{A}	17 ± 3^{B}	23 ± 1^{ABC}	21 ± 1^{AB}

Table 4 Average current density (I_{ave}), COD removal rate (COD_{rr}), coulombic efficiency (CE) and maximum current density (I_{max}) in the MFCs using different external resistance (R_{ext}) and substrate loading (L_{sub}).

Batch No.	R_{ext} [Ω]	L_{sub} [g·dm^{-3}]	I_{ave} [mA·m^{-2}]	I_{max} [mA·m^{-2}]	COD_{rr} [g·m^{-3}·day^{-1}]	CE [%]
Cycle 3	200	1	555 ± 8	1780 ± 0.03	152 ± 1	58 ± 1
	500	1	272 ± 4	990 ± 0.01	112 ± 2	38 ± 1
	800	1	180 ± 2	860 ± 0.01	110 ± 3	26 ± 1
	1000	1	145 ± 10	570 ± 0.01	92 ± 6	25 ± 2
Cycle 4	200	1	557 ± 13	1800 ± 0.02	150 ± 10	59 ± 1
Cycle 5	200	0.5	419 ± 28	1820 ± 0.06	111 ± 1	61 ± 2
	200	1	559 ± 10	1810 ± 0.05	149 ± 2	60 ± 1
	200	1.5	557 ± 10	1780 ± 0.05	187 ± 3	47 ± 1
	200	2	553 ± 12	1780 ± 0.04	188 ± 6	47 ± 1

Note: all four MFCs in cycle 4 were changed to use same R_{ext} and L_{sub} with similar performance.

Table 5 DGGE 16S rRNA gene band identification and characterisation of the species

Band	Accession no.	Gene bank match	Identity [%]	Ref.	Characteristics
1	LN651010	*Bacteroides graminisolvens*	91	[22]	Strict anaerobe fermenting xylan /xylose
2	LN651006	*Arcobacter butzleri*	100	[23]	Facultative anaerobe detected on meet/food
3	LN651030	*Paludibacter propionicigenes*	84	[24]	Strict anaerobe fermenting sugars to propionate
4	LN651003	*Thermanaerovibrio acidaminovorans*	87	[25]	Fermenting anaerobic bacterium
5	LN651037	*Shigella flexneri*	99		Facultative anaerobe failing to ferment lactose or decarboxylate lysine
6	LN651061	Uncultured bacterium	92		
7	LN651020	*Enterobacter cancerogenus*	99	[26]	Facultative anaerobes fermenting glucose
8	LN651027	*Geobacter sulfurreducens*	99	[5]	Metal-reducing anaerobe oxidizing short-chain fatty acids, alcohols, and monoaromatic compounds with the ability to generate electricity
9	LN651013	*Citrobacter braakii*	99	[27]	Facultative anaerobe solely fermenting lactose
10	LN651053	*Propionispora hippei*	91	[28]	Strict anaerobe fermenting sugars to acetate and propionate
11	LN651007	*Azonexus caeni*	100		Nitrogen-fixing bacteria

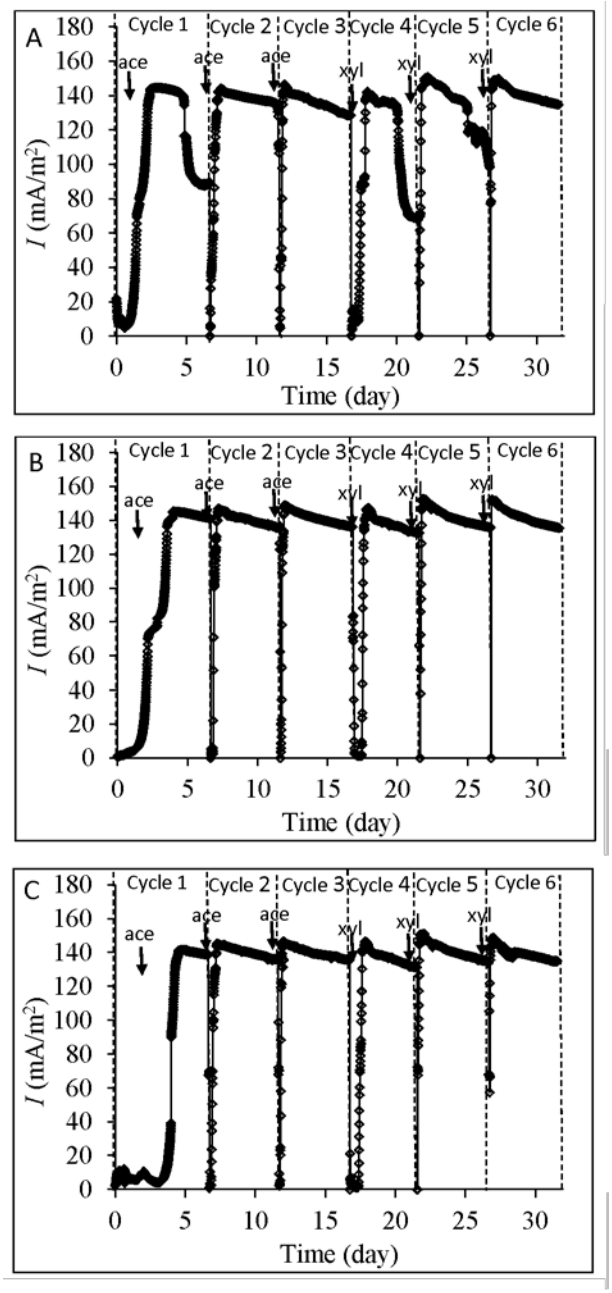
A
B
C
Cycle 1
Cycle 2
Cycle 3
Cycle 4
Cycle 5
Cycle 6
ace
xyl
I (mA/m2)
Time (day)

Figure 1

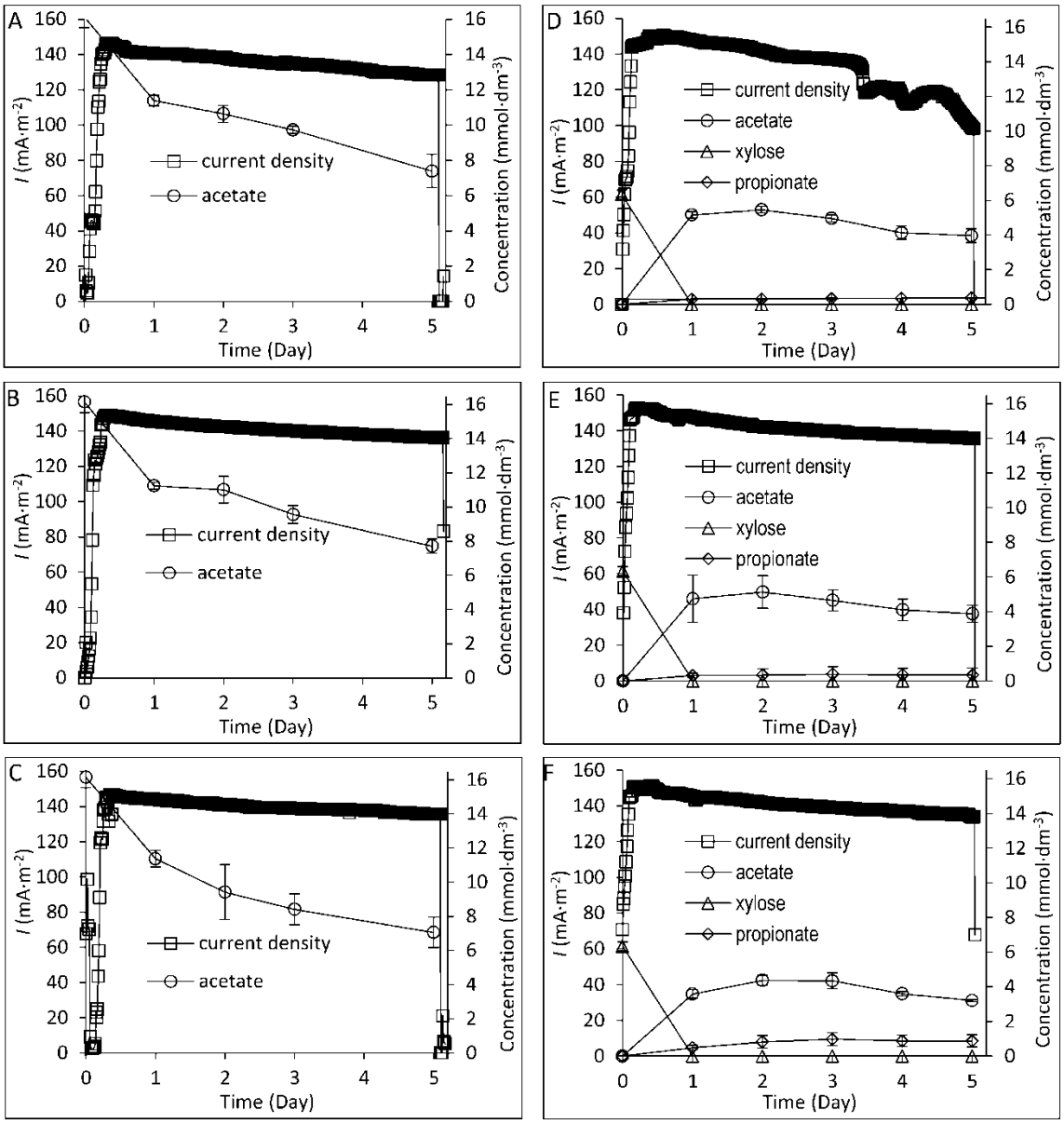
A
B
C
D
E
F
I (mA·m-2)
Concentration (mmol·dm-3)
Time (Day)
current density
acetate
xylose
propionate

Figure 2

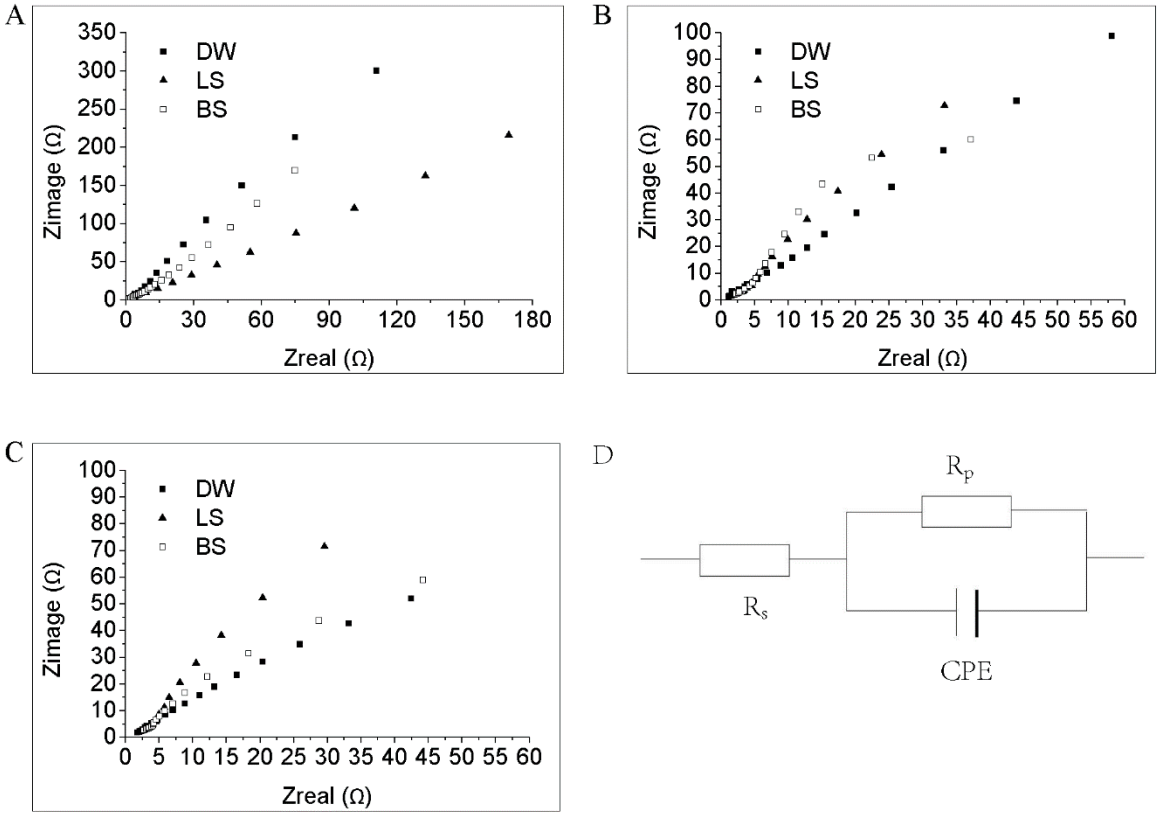

Figure 3

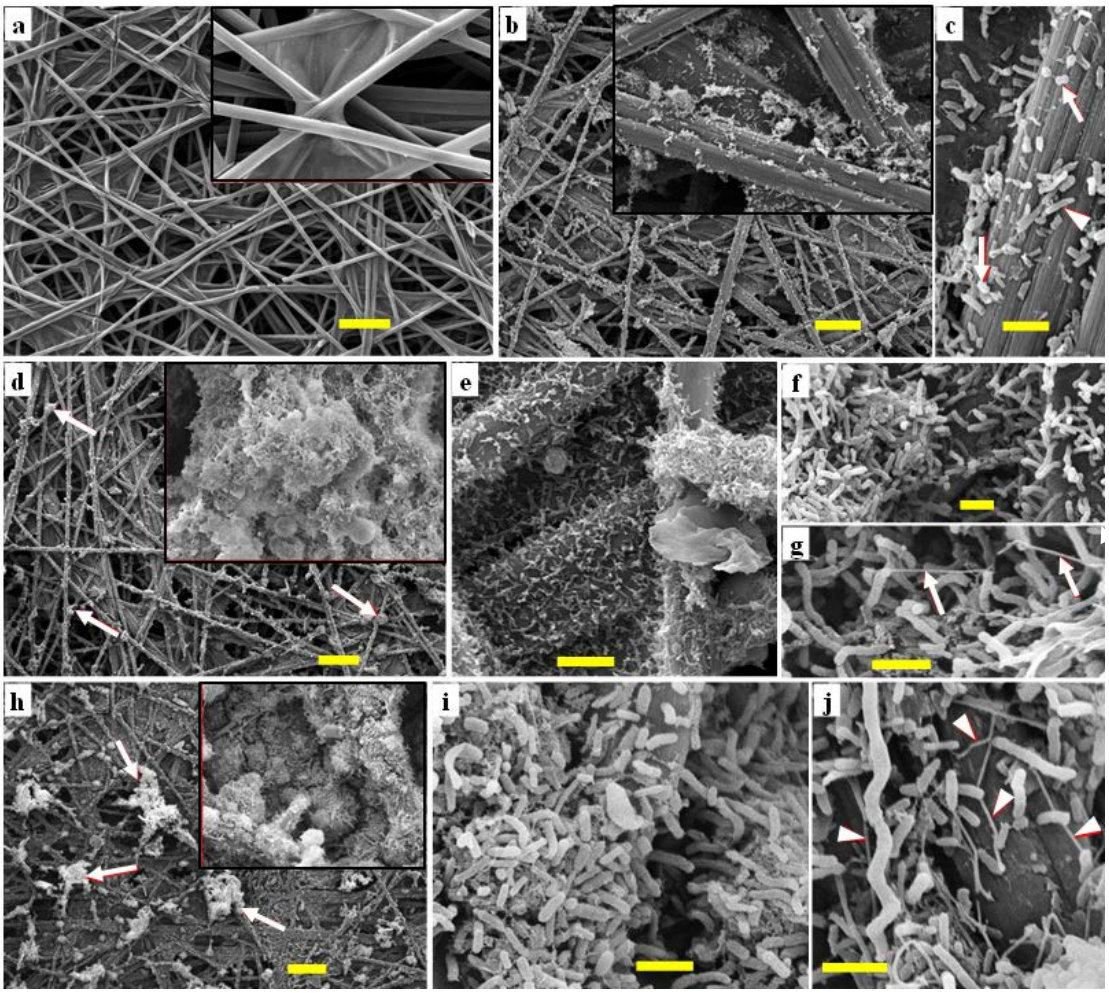

Figure 4

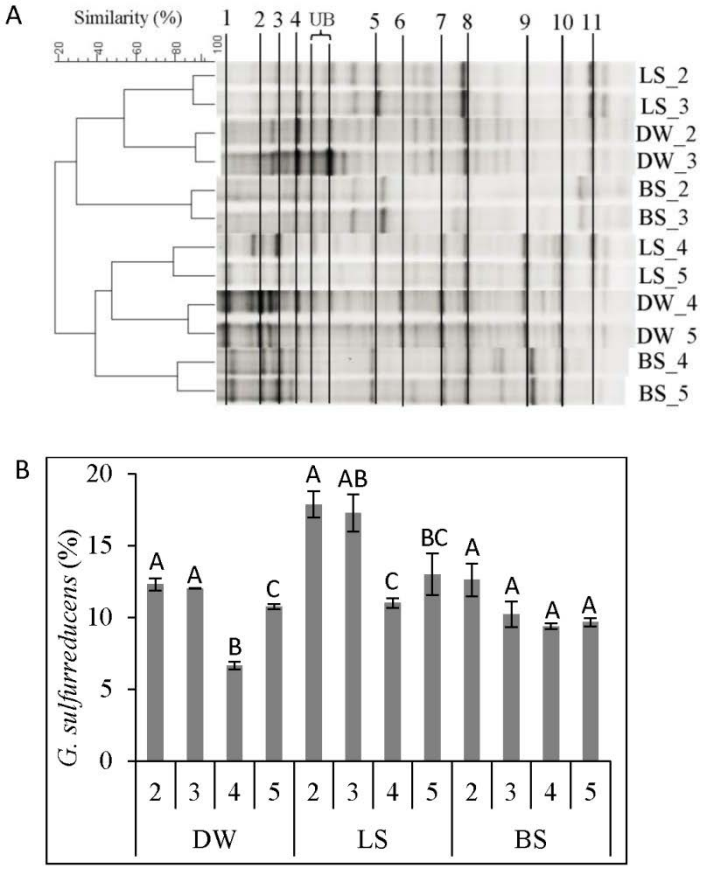
A
Similarity (%)
20
40
60
80
100
1 2 3 4 UB 5 6 7 8 9 10 11
LS_2
LS_3
DW_2
DW_3
BS_2
BS_3
LS_4
LS_5
DW_4
DW_5
BS_4
BS_5
B
G. sulfurreducens (%)
20
15
10
5
0
A A B C A AB C BC A A A A
2 3 4 5 2 3 4 5 2 3 4 5
DW
LS
BS

Figure 5

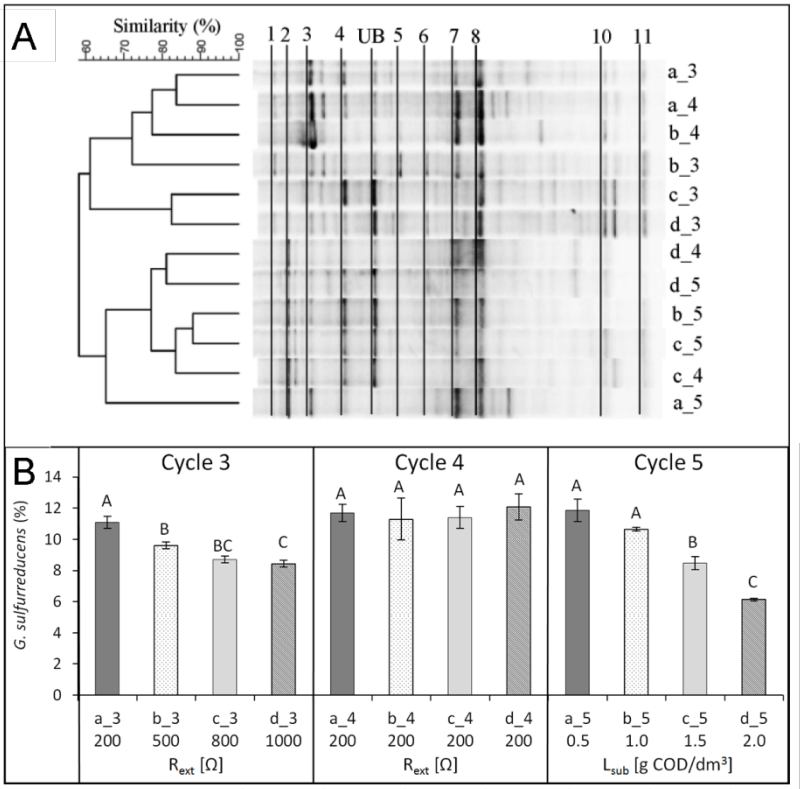
A
Similarity (%)
60
70
80
90
100
1 2 3 4 UB 5 6 7 8 10 11
a_3
a_4
b_4
b_3
c_3
d_3
d_4
d_5
b_5
c_5
c_4
a_5
B
G. sulfurreducens (%)
Cycle 3
Cycle 4
Cycle 5
a_3 200
b_3 500
c_3 800
d_3 1000
a_4 200
b_4 200
c_4 200
d_4 200
a_5 0.5
b_5 1.0
c_5 1.5
d_5 2.0
R_ext [Ω]
R_ext [Ω]
L_sub [g COD/dm³]

Figure 6

Graphic abstract: